

## Vapor Phase Self-Assembly of Molecular Gate Dielectrics for Thin Film Transistors

Sara A. DiBenedetto, David Frattarelli, Mark A. Ratner,\* Antonio Facchetti,\* and Tobin J. Marks\*

Department of Chemistry and the Materials Research Center, Northwestern University, 2145 Sheridan Road, Evanston, Illinois 60208

Received February 21, 2008; E-mail: ratner@northwestern.edu; a-facchetti@northwestern.edu; t-marks@northwestern.edu

Small molecule and polymeric dielectric thin films with large permittivities ( $k$ ) have recently found applications in organic field effect transistors (OFETs), where replacing the traditional  $\text{SiO}_2$  gate dielectric with high capacitance materials enables lower operating voltages, reduced power consumption, and improved performance.<sup>1</sup> The gate dielectric capacitance  $C_g$  in an OFET can be described by a parallel plate capacitor, where  $C_g = \epsilon_0 k d$  ( $d$  = the thickness, and  $\epsilon_0$  = the permittivity of vacuum). To achieve large capacitances, it is necessary to reduce the thickness and/or increase the dielectric film permittivity. This approach offers an intriguing materials challenge not only because small molecule and polymeric materials with large permittivities (i.e.,  $\pi$ -conjugated) are usually poor insulators but also because as the insulator film thickness is reduced, concurrent leakage current increases can degrade OFET performance.<sup>2</sup>

Dielectric materials composed of molecular components are ideal candidates for OFETs because small molecules have nanometer length scales, tunable electronic structures, processability on flexible substrates, and are compatible with organic semiconductors.<sup>3</sup> Previously, we demonstrated the application of molecular self-assembled nanodielectrics (SANDs) as gate dielectrics. SAND films are fabricated via a layer-by-layer solution phase self-assembly of  $\sigma$ - $\pi$  organosilane precursors to yield hybrid organic-inorganic multilayers.<sup>4</sup> Here the highly polarizable  $\pi$ -conjugated component is a stilbazolium group (Stb). An interesting question is whether similar hybrid films based on highly  $\pi$ -polarizable components can be fabricated from the vapor phase in a “dry” process that does not involve multistep “wet” organosilane self-assembly. In this contribution, we demonstrate that SAND-like organic-inorganic films for OFET gate dielectrics can be fabricated entirely via vapor-phase processing (v-SAND). Pentacene OFETs based on v-SANDs exhibit excellent performance at low operating voltages, demonstrating a new approach to high- $k$  organic gate dielectrics.

New v-SAND  $\pi$ -conjugated building blocks **1** and **2** were designed to form robust self-ordered thin films via head-to-tail intramolecular hydrogen-bonding (Figure 1A). In addition, the  $\pi$ -conjugated organic donor-acceptor functionalities should enhance the electronic polarizability needed to achieve a high- $k$  bulk layer. The molecular geometries of **1** and **2** were optimized using DFT/B3LYP density functional theory and a 6-31G\*\* basis set in Jaguar v5.00.22 using the Maestro Molecular Modeling Interface c5.10.20. Molecular polarizabilities in the  $z$ -direction ( $\alpha_z$ , parallel to the molecular long axis, Figure 1A) were calculated using INDO(SOS).<sup>5</sup> The computed polarizabilities of **1** ( $176 \times 10^{-24} \text{ cm}^3$ ) and **2** ( $70.2 \times 10^{-24} \text{ cm}^3$ ) are, respectively, larger than and comparable to that of Stb in SAND ( $91.3 \times 10^{-24} \text{ cm}^3$ ). Classic dielectric theory relates molecular polarizability to bulk dielectric permittivity through the Clausius-Mossotti relationship,  $k \propto (3 + 2\alpha_z N)/(3 - \alpha_z N)$  where  $N$  is the molecular density (molecules/ $\text{cm}^3$ ).<sup>6</sup> Accordingly, it is expected that the larger polarizabilities of **1** and **2** and the greater molecular densities afforded by vapor

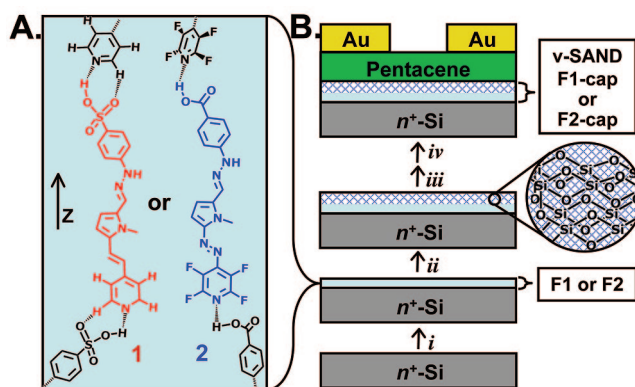


**Figure 1.** (A) Chemical structures of **1** and **2**, and (B) OFET device fabrication: (i) vapor deposition of **1** or **2**, (ii) exposure of **F1** or **F2** to  $\text{Cl}_3\text{Si-O-SiCl}_3$  vapors, completing the v-SAND structure, (iii) vapor deposition of pentacene (50 nm), and (iv) vapor deposition of Au electrodes through a shadow mask to complete the OFET device.

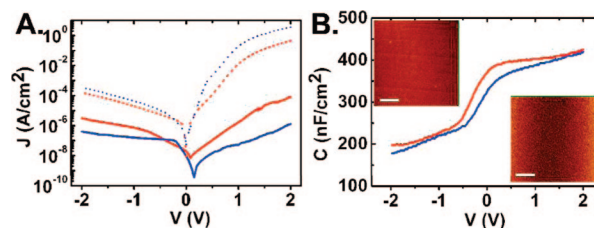


**Figure 2.** (A) Leakage current density versus voltage plots for **F1** (red dotted line), **F2** (blue dotted line), **F1-cap** (red solid line), and **F2-cap** (blue solid line) films. (B) Capacitance versus voltage plots for **F1-cap** (red) and **F2-cap** (blue) films. Inset (top): AFM image of **F1** on Si. Inset (bottom): AFM image of **F1-cap**. The scale bar is  $2 \mu\text{m}$ .

phase versus solution-deposited film growth techniques should translate into higher  $k$ 's.<sup>7</sup>

Compounds **1** and **2** were synthesized following procedures reported in Supporting Information and were characterized by conventional analytical/spectroscopic techniques. v-SAND films are fabricated according to the scheme in Figure 1B and are composed of a bottom layer of either **1** or **2** and capped with a top  $\text{SiO}_x$  “capping layer.” Films of **1** and **2** (**F1** and **F2**, respectively) were vapor-deposited at a rate of  $0.2 \text{ \AA/s}$  onto solvent-cleaned<sup>8</sup> heavily doped  $n^+$ -Si substrates at  $10^{-6}$  Torr. To deposit the  $\text{SiO}_x$  capping layer, **F1** and **F2** were exposed to hexachlorodisiloxane ( $\text{Cl}_3\text{Si-O-SiCl}_3$ ) vapors under  $\text{N}_2$  for 20 min and then annealed under vacuum (20 Torr) at  $110 \text{ }^\circ\text{C}$  to afford **F1-cap** and **F2-cap**, respectively (see Figure S1 for the apparatus). AFM images (Figures 2 and S2) of the uncapped and capped films demonstrate smooth surface morphologies (maximum rms roughness  $\sim 0.5 \text{ nm}$ ) that is important for optimal OFET performance.<sup>9</sup> Optical spectra of the films on glass before and after  $\text{SiO}_x$  deposition (Figure S3) exhibit

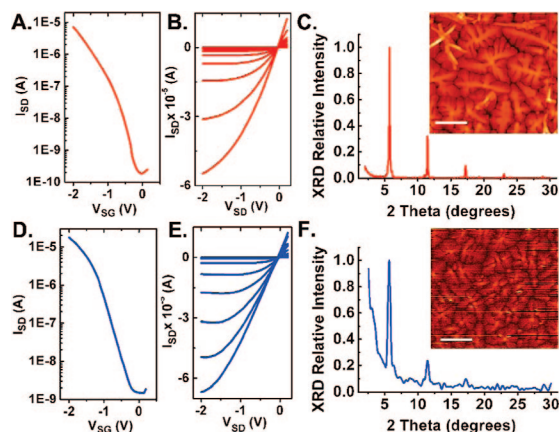


**Figure 3.** Transfer (A and D) and output (B and E) plots for pentacene OFETs based on v-SANDs of **F1-cap** (top) and **F2-cap** (bottom). AFM images and XRD spectra of the corresponding 50 nm thick pentacene films grown on **F1-cap** (C) and **F2-cap** (F).

only minor differences, arguing that the capping reagent does not react with the underlying **F1** or **F2** molecular layer but is simply deposited on top.

To assess v-SAND dielectric properties, metal–insulator–semiconductor devices were fabricated by depositing Au electrodes ( $200 \times 200 \mu\text{m}^2$ ) on both the all-organic **F1** and **F2** films as well as on the organic–inorganic **F1-cap** and **F2-cap** films. As in the case of solution processed SANDs,<sup>4a</sup> a substantial leakage current density ( $J_{\text{leak}}$ ) reduction is observed ( $10\text{--}10^{-2}$  to  $10^{-5}\text{--}10^{-7}$  A/cm<sup>2</sup> at 2 V) after capping layer deposition (**F1**, **F2** → **F1-cap**, **F2-cap**). The suppressed leakage current indicates that the capping functions as an efficient electron tunneling barrier.<sup>10</sup>

Because of the large **F1** and **F2**  $J_{\text{leak}}$  values, meaningful capacitances are only measurable for **F1-cap** and **F2-cap** and are found to be  $\sim 400$  nF/cm<sup>2</sup> at 2 V (Figure 2). Permittivities of the v-SAND organic components can be estimated by modeling **F1-cap** and **F2-cap** dielectric layers as three parallel plate capacitors in series (Si native oxide + **F1** or **F2** + SiO<sub>x</sub>). The capping layer thickness is  $\sim 5.9$  nm, and the organic layer thicknesses are  $\sim 3.6$  nm (by X-ray reflectivity, Figure S4). Using the accumulation regime capacitances of **F1-cap** (400 nF/cm<sup>2</sup>) and **F2-cap** (390 nF/cm<sup>2</sup>),  $k$  values of  $\sim 11$  and  $\sim 9$  are estimated for **F1** and **F2**, respectively ( $d_{\text{native oxide}} = 1.5$  nm, and  $k_{\text{native oxide}} = k_{\text{capping layer}} = 3.9$ ). The larger  $k$  of **F1** versus that of **F2** is anticipated by the INDO(SOS) computation of the molecular  $\alpha_z$  values in the context of the aforementioned Clausius–Mossotti equation and can be explained by the greater acidity of **1**, which enhances the molecular zwitterionic character upon intermolecular hydrogen bonding.

Given the excellent v-SAND dielectric properties, bottom-gate top-contact OFETs were fabricated by vapor deposition of pentacene on the v-SAND films, and the  $I$ – $V$  characteristics were analyzed by standard procedures.<sup>11</sup> Using the above capacitances and channel dimensions ( $L = 200 \mu\text{m}$  and  $W = 5000 \mu\text{m}$ ), these OFETs exhibit excellent performance with hole mobilities of  $1.9 \pm 0.3$  and  $2.4 \pm 0.3$  cm<sup>2</sup>/V·s for the **F1-cap** and **F2-cap** based devices, respectively,  $I_{\text{on}}/I_{\text{off}} \sim 10^5$ , and  $V_T \sim 1$  V. Note that  $I$ – $V$  output plots at each gate voltage intersect at the origin, indicating very low gate leakage during device operation (Figure 3). OFETs tested after 4 months from fabrication exhibit small performance erosion with  $\mu'$ s decreased by  $\sim 10$  and  $\sim 30\%$  for the devices based on **F2-cap** and **F1-cap**, respectively (see Figure S6). These results demonstrate that vapor-phase deposition can profitably utilize and probe the dielectric response properties of high- $k$  molecular layers without compromising the insulating properties of the resulting hybrid films and, furthermore,

have larger mobilities at lower operating voltages than OFETs with pentacene fabricated on 300 nm SiO<sub>2</sub> (Figure S5). To understand the origin of the large carrier mobilities, AFM images and XRD spectra of the pentacene films on top of v-SANDs were acquired (Figure 3). Very large pentacene crystal grains ( $\sim 2\text{--}3 \mu\text{m}$ ) are observed by AFM, which are comparable to or larger than those in other high-mobility OFETs.<sup>12</sup> In addition, the XRD spectra demonstrate highly textured pentacene films having the thin film phase crystal structure ( $d$  spacing = 15.4 Å on both v-SANDs).<sup>12</sup>

In summary, we have demonstrated a straight forward, vapor-phase approach for fabricating self-assembled nanodielectrics (v-SANDs) exhibiting substantial capacitances and excellent insulating properties. Pentacene OFETs based on **F1-cap** and **F2-cap** exhibit very large mobilities.

**Acknowledgment.** This work was supported by the NSF MRSEC program (DMR-0520513) at the Materials Research Center of Northwestern University, and by the ONR MURI Program (N00014-02-1-0909).

**Supporting Information Available:** Synthesis of **1** and **2**, film/device fabrication details, and AFM/optical/XRR/OFET data. This material is available free of charge via the Internet at <http://pubs.acs.org>.

## References

- (1) (a) Katz, H. E.; Hong, M.; Dodabalapur, A. *J. Appl. Phys.* **2002**, *91*, 1572. (b) Podzorov, V.; Pudalov, V. M.; Gershenson, M. E. *Appl. Phys. Lett.* **2003**, *82*, 1739. (c) Majewski, L. A.; Schroeder, R.; Grell, M. *J. Phys. D: Appl. Phys.* **2004**, *37*, 21. (d) Park, Y. D.; Kim, D. H.; Jang, Y.; Hwang, M.; Lim, A. L.; Cho, K. *Appl. Phys. Lett.* **2005**, *87*, 243509. (e) Yang, S. Y.; Kim, S. H.; Shin, K.; Jeon, H.; Park, C. E. *Appl. Phys. Lett.* **2006**, *88*, 173507. (f) Onoue, T.; Nakamura, I.; Sakabe, Y.; Yasuda, T.; Tsutsui, T. *Jpn. Soc. Appl. Phys.* **2006**, *45*, L770. (g) Singh, B.; Sariciftci, N. S. *J. Appl. Phys.* **2006**, *100*, 024514. (h) Klauk, H.; Zschieschang, U.; Pfau, J.; Halik, M. *Nature* **2006**, *445*, 745. (i) McDowell, M.; Hill, I. G.; McDermott, J. E.; Bernasek, S. L.; Schwartz, J. *Appl. Phys. Lett.* **2006**, *88*, 073505. (j) Kim, C. S.; Jin, S.; Lee, S. W.; Kim, W. J.; Bail, H. K.; Lee, S. J.; Hwang, D. K.; Im, S. *Appl. Phys. Lett.* **2006**, *88*, 243515. (k) Jeong, Y. T.; Dodabalapur, A. *Appl. Phys. Lett.* **2007**, *91*, 193509. (l) Lee, J.; Panzer, M. J.; He, Y.; Lodge, T. P.; Frisbie, C. D. *J. Am. Chem. Soc.* **2007**, *129*, 4532.
- (2) Devine, R. A. B.; Busani, T. *Appl. Phys. Lett.* **2005**, *86*, 062902.
- (3) (a) Veres, J.; Ogier, S.; Lloyd, G.; de Leeuw, D. *Chem. Mater.* **2004**, *16*, 4543. (b) Weitz, R. T.; Zschieschang, U.; Effenberger, F.; Klauk, H.; Burghard, M.; Kern, K. *Nano. Lett.* **2007**, *7*, 22. (c) Collet, J.; Tharaud, O.; Chapon, A.; Vuillaume, D. *Appl. Phys. Lett.* **2000**, *76*, 1941.
- (4) (a) Yoon, M.-H.; Facchetti, A.; Marks, T. J. *Proc. Natl. Acad. Sci. U.S.A.* **2005**, *102*, 4678. (b) Ju, S.; Lee, K.; Janes, D. B.; Yoon, M.-H.; Facchetti, A.; Marks, T. J. *Nano. Lett.* **2005**, *5*, 2281. (c) Hur, S.-H.; Yoon, M.-H.; Gaur, A.; Facchetti, A.; Marks, T. J. *J. Am. Chem. Soc.* **2005**, *127*, 13808. (d) Ju, S.; Lee, K.; Yoon, M.-H.; Facchetti, A.; Marks, T. J.; Janes, D. B. *Appl. Phys. Lett.* **2006**, *89*, 073510. (e) Ju, S.; Lee, K.; Yoon, M.-H.; Facchetti, A.; Marks, T. J.; Janes, D. B. *Nanotechnol.* **2007**, *18*, 155201. (f) Lin, H. C.; Ye, P. D.; Xuan, Y.; Lu, G.; Facchetti, A.; Marks, T. J. *Appl. Phys. Lett.* **2006**, *89*, 14210. (g) Ju, S.; Janes, D. B.; Lu, G.; Facchetti, A.; Marks, T. J. *Appl. Phys. Lett.* **2006**, *89*, 193506. (h) Wang, L.; Yoon, M.-H.; Facchetti, A.; Marks, T. J. *Adv. Mater.* **2007**, *19*, 3252.
- (5) Keinan, S.; Ratner, M. A.; Marks, T. J. *Chem. Phys. Lett.* **2006**, *417*, 293.
- (6) (a) Rohleder, J. W.; Munn, R. W. *Magnetism and Optics of Molecular Crystals*; Wiley: New York, 1992. (b) Yamada, K.; Saiki, A.; Sakaue, H.; Shingubara, S.; Takahagi, T. *Jpn. J. Appl. Phys.* **2001**, *40*, 4829.
- (7) (a) Typical  $N$  values of self-assembled siloxane-based chromophores are  $\sim 10^{20}$  molecules/cm<sup>3</sup> (ref 7b), while vapor deposition  $N$  values are typically  $\sim 10^{21}$  molecules/cm<sup>3</sup> (ref 7c). (b) Roscoe, S. B.; Yitzchaik, S.; Kakkar, A. K.; Marks, T. J.; Xu, Z.; Zhang, T.; Lin, W.; Wong, G. K. *Langmuir* **1996**, *12*, 5338. (c) Choubey, A.; Kwon, O.-P.; Jazbinsek, M.; Günter, P. *Cryst. Growth Des.* **2007**, *7*, 402.
- (8) Kim, C.; Facchetti, A.; Marks, T. J. *Adv. Mater.* **2007**, *19*, 2561.
- (9) Steudel, S.; Vusser, S. D.; Jonge, S. D.; Janssen, D.; Verlaak, S.; Genoe, J.; Heremans, P. *Appl. Phys. Lett.* **2004**, *85*, 4400.
- (10) (a) McBrayer, J. D.; Swanson, R. M.; Sigmund, T. W. *J. Electrochem. Soc.* **1986**, *133*, 1242. (b) Huntley, F. A.; Willoughby, A. F. W. *Solid-State Electron.* **1970**, *14*, 641. (c) Bal, J. K.; Hazra, S. *Phys. Rev. B* **2007**, *75*, 205411. (d) Dubois, G.; Volksen, W.; Magbitang, T.; Miller, R. D.; Gage, D. M.; Dauskardt, R. H. *Adv. Mater.* **2007**, *19*, 3989.
- (11) Newman, C. R.; Frisbie, C. D.; da Silva Filho, D. A.; Bredas, J.-L.; Ewbank, P. C.; Mann, K. R. *Chem. Mater.* **2004**, *16*, 4436.
- (12) (a) Yang, H.; Shin, T. J.; Ling, M.-M.; Cho, K.; Ryu, C. Y.; Bao, Z. *J. Am. Chem. Soc.* **2005**, *127*, 11542. (b) Kim, C.; Facchetti, A.; Marks, T. J. *Science* **2007**, *318*, 76.

JA801309G